Morphometrics and genetics highlight the complex history of Eastern Mediterranean spiny mice

SABRINA RENAUD [1]*, EMILIE A. HARDOUIN [2], PASCALE CHEVRET [1], KATERINA PAPAYIANNIS [3,4], PETROS LYMBERAKIS [5], FERHAT MATUR [6], OXALA GARCIA-RODRIGUEZ [2], DEMETRA ANDREOU [2], ORTAÇ ÇETINTAŞ [7], MUSTAFA SÖZEN [7], ELEFTHERIOS HADJISTERKOTIS [8], GEORGE P. MITSAINAS [9]

[1] Laboratoire de Biométrie et Biologie Evolutive, UMR5558, CNRS, Université Claude Bernard Lyon 1, Université de Lyon, Campus de la Doua, 69100 Villeurbanne, France

[2] Department of Life and Environmental Sciences, Faculty of Science and Technology, Bournemouth University, Christchurch House, Talbot Campus, Poole, Dorset BH12 5BB, U.K.

[3] Archéozoologie – Archéobotanique, Société, Pratiques et Environnements (ASPE), UMR 7209 CNRS, Muséum National d'Histoire Naturelle, 55 rue Buffon, 75005 Paris, France

[4] Present address: Department of History and Archaeology, National and Kapodistrian University of Athens, Greece

[5] Natural History Museum of Crete, University of Crete, Heraklion Crete, Greece

[6] Dokuz Eylül University, Faculty of Science, Department of Biology, Buca, 35412, Izmir, Turkey

[7] Zonguldak Bulent Ecevit University, Department of Biology, Zonguldak, Turkey

[8] Agricultural Research Institute, P.O. Box 22016, 1516, Nicosia, Cyprus

[9] Section of Animal Biology, Department of Biology, University of Patras, 26500 Patras, Greece

* Corresponding author

Short running title:

Acomys cahirinus in the Eastern Mediterranean area

Abstract

Spiny mice of the *Acomys cahirinus* group display a complex geographic structure in the Eastern Mediterranean area, as shown by former genetic and chromosomal studies. In order to better elucidate the evolutionary relationships of insular populations from Crete and Cyprus with the continental ones from North Africa and Cilicia in Turkey, genetic and morphometric variations were investigated, based on mitochondrial D-loop sequences, and size and shape of the first upper molar. The Cypriot and the Cilician populations show idiosyncratic divergence in molar size and shape, while Crete presents a geographic structure with at least three differentiated sub-populations, as shown by congruent distributions of haplogroups, Robertsonian fusions and morphometric variation. A complex history of multiple introductions is most probably responsible for this structure, and insular isolation coupled with habitat shift should have further promoted a pronounced and rapid morphological evolution in molar size and shape on Crete and Cyprus.

Keywords

Acomys minous; Acomys cilicicus; Acomys nesiotes; Crete; Cyprus; D-loop; geometric morphometrics; insular evolution; molar shape; phylogeography.

Introduction

Spiny mice of the genus *Acomys* occupy a large distribution area over Africa to Western Asia, including a small area along the Mediterranean coast of Turkey, a region historically known as Cilicia. They further occur on the islands of Crete and Cyprus, within the Eastern Mediterranean area, which along with Cilicia, constitute the northernmost distribution limit of the genus. The lack of clear diagnostic characters led to a taxonomic debate within a group of closely related species known as the *cahirinus-dimidiatus* group (Denys et al., 1994; Volobouev et al., 2007; Frynta et al., 2010; Aghová et al., 2019). A growing body of genetic and chromosomal evidence showed that one clade, attributed to *A. dimidiatus*, nowadays occupies the Levant, including Israel and Sinai, up to Arabia and Iran. The other clade (*A. cahirinus*) would only occur between Eastern Sahara and Egypt along the Nile Valley (Volobouev et al., 2007; Frynta et al., 2010). Spiny mice from Crete, Cyprus and Cilicia are affiliated to the second group (Barome et al., 2001; Frynta et al., 2010; Giagia-Athanasopoulou et al., 2011). Being considered endemics, and some of them displaying distinct morphological features, such as a larger body size (Kryštufek & Vohralík, 2009), each of these populations was given a specific or subspecific status: *A. nesiotes* for the Cypriot, *A. cilicicus* for the Cilician, and *A. minous* for the Cretan populations. Crete, however, is characterized by genetic heterogeneity, with the co-existence of two distinct mitochondrial clades, one also found in Cyprus and the low Nile valley (Cairo, Egypt), and the other one in Cilicia (Barome et al., 2001) and the high Nile Valley, Libya, and Chad (Frynta et al., 2010). Cretan mice further vary in their chromosomal number, which ranges from 2*n*=38 to 2n=42, due to Robertsonian fusions. No individual association has been found between the chromosomal number and the mitochondrial lineage (Giagia-Athanasopoulou et al., 2011).

In order to better understand the evolutionary history of the *cahirinus* "*sensu lato"* group (including *A. minous, A. nesiotes* and *A. cilicicus*), a geometric morphometric analysis of the first upper molar (Fig. 1) was performed. In *Acomys* as in murine rodents, the first molar erupts before weaning and is subsequently affected only by wear. Molar shape differences are thus indicative of underlying genetic changes. In contrast, osteological characters, such as skull or mandible, are prone to plastic remodelling along an animal's life and consequently, they also vary on a short time-scale, depending on local ecological conditions (Caumul & Polly, 2005; Ledevin et al., 2012). Furthermore, molar teeth are the most frequent fossil remain of small mammals; their study allows a comparison of modern and ancient samples, providing a temporal perspective. Hence, the morphometric analysis of molar shape may deliver valuable insight on the genetic differentiation among populations, complementary to the analysis of mitochondrial DNA for which the existing data were supplemented with new mitochondrial D-loop sequences from Crete, Cyprus and Cilicia.

Based on these morphometric and genetic data, the following questions were addressed: (1) Is the genetic and chromosomal heterogeneity on Crete mirrored in a high morphological disparity? (2) Can a synthesis of the genetic, morphometric and chromosomal data shed light on the processes that led to the diversity within *Acomys cahirinus s.l.* in the Eastern Mediterranean area? (3) Insularity is known to trigger rapid morphological divergence (Millien, 2006). If drift in isolated populations is the dominant factor, a pronounced morphological divergence is expected in Cilicia, as on the islands of Crete and Cyprus. If adaptation to island-specific ecological conditions, including changes in the level of competition and predation, is the prime driving factor of divergence (Lomolino, 1985, 2005), the Cilician population should display less divergence compared to those of Crete and Cyprus.

Material

Sampling for genetics

Thirty new D-loop sequences were acquired, including specimens from Cyprus, Crete, and Cilicia (Table 1): (1) Five Cypriot specimens ("*A. nesiotes*") collected in 2015. Despite a sampling effort around the island, specimens were only caught on Cap Greco or adjacent to it. (2) Eleven Cretan specimens ("*A. minous*"). (3) Fourteen Cilician individuals ("*A. cilicicus*") trapped in spring 2013, around Narlıkuyu, in the district of Mersin (Turkey).

Sampling for morphometrics

The morphometric study (Table 1) included 92 specimens collected in Crete (61), Cyprus (6), and Cilicia (17). This sampling was complemented by eight specimens from Cairo (Egypt) from the Museum National d'Histoire Naturelle de Paris (vouchers: 2001-11; 1997-1308; 1996-432; 1996-446; 1996-431; 1996-430; 1994-1280; 1999-6), identified as *A. cahirinus*.

Four other specimens from the Museum National d'Histoire Naturelle de Paris were attributed with less certainty to *A. cahirinus*, but coming from Sudan and Chad, they allowed to document the geographic variation at a larger scale (vouchers: 1906-118a; 1906-118b; 1906-118c; 1981-1059).

Body size and sex data were available for most specimens, allowing to investigate the occurrence of sexual dimorphism and allometry. All specimens were identified as sub-adult or adult, based on the criterion of the eruption of the third molars. One specimen from Cairo (Egypt) was a juvenile, since its third molars were not erupted. It was not included in the analyses of body size, but since the

molar does not grow further after its eruption, it was included in the analyses of first molar size and shape.

Finally, three fossil teeth from the floor of the Hellenistic Temple C at the ancient port of Kommos on the south coast of Crete, dated between 375 B.C. and AD 160/170 (Shaw, 2000), were measured based on drawings of published plates (Payne, 1995) and included in the morphometric analyses.

Methods

Genetic analyses

Acomys tissue samples were extracted using DNEasy from Qiagen following the manufacturer instructions. A D-loop fragment of 514 bp was amplified using previously described primers (Nicolas et al., 2009). PCR conditions were as follows: 10ng of DNA, 2mM of MgCl2, 0.2mM dNTP, 0.5U of Taq, 0.2 µM of each primer. PCR cycles were 15 min 95°C, followed by 35 cycles with 30 sec at 95°C, 1:30 min at 54°C, 1 min at 72°C; final elongation was 15 min at 72°C. The sequences generated were visualized and analyzed CLC Workbench (Qiagen) and aligned with Seaview v4 (Gouy et al., 2010). Genetic diversity indices were calculated using DNAsp (Librado & Rozas, 2009).

A phylogenetic tree was generated using MrBayes (Ronquist et al., 2012) and PhyMl 3.0 (Guindon et al., 2010), including the 30 sequences generated in the present study and the 16 sequences available from GenBank, leading to a total of 46 sequences of *A. cahirinus s.l.*. The haplotypes were determined with DNAsp (Librado & Rozas, 2009). Only the 20 haplotypes differing by mutation were retained for the phylogenetic analysis. We added to these haplotypes seven *A. dimidiatus* (AJ012028, MH044889, MH044888, MH044871, MH044868, MH044840, FJ415545) as well as three *A. ignitus* (MH044872, MH044875, MH044876), two *A. wilsoni* (MH044862, MH044874) and three *A. russatus* (MH044881, MH044885 and FJ415546) that were used as outgroups. The sites with more than 20% missing data were removed and the final alignment comprised 35 sequences and 493 sites. The substitution model, GTR+I+G, was chosen using jmodeltest (Darriba et al., 2012). Robustness of the nodes was estimated with 1000 bootstrap replicates with PhyMl and posterior probability with MrBayes. The generation number was set at 2000000 MCMC with one tree sampled every 500 generations. The burn-in was graphically determined with Tracer v1.7 (Rambaut et al., 2018). We also checked that the effective sample sizes (ESSs) were above 200 and that the average standard deviation of split frequencies remained <0.01 after the burn-in threshold. We discarded 20% of the trees and visualized the resulting tree with Figtree v1.4 (Rambaut, 2012). A median-joining haplotype network was constructed in PopART (Leigh & Bryant, 2015) with the 46 *A. cahirinus* sequences only.

All the sequences generated in the present study are available on GenBank (GenBank numbers MT001830-MT001858, MT043301) (Table 1).

To estimate the divergence time of the lineages of *A. cahirinus* in the Eastern Mediterranean area, we used BEAST v 2.5.2 (Bouckaert et al., 2019), including its functions BEAUTI, LogCombiner and TreeAnotator. The mitochondrial (Cyt *b* + D-loop) and nuclear genes (IRBP, RAG1) were retrieved from GenBank for 32 *Acomys* representing the main lineages within this genus (Aghová et al., 2019) and 4 outgroups (*Deomys ferrugineus, Lophuromys flavopunctatus, Lophuromys sikapusi* and *Uranomys ruddi*) (Supp. Table 1). The two Eastern Mediterranean lineages were each represented by one specimen for which sequences of the four genes were available (Supp. Table 1). The dataset comprised 36 sequences and 3509 bp. The best partitioning scheme and substitution models were determined with PartitionFinder 2 (Lanfear et al., 2017) using a greedy heuristic algorithm with 'linked branch lengths' option and the Bayesian Information Criterion (BIC) (Supp. Table 2). The partitions were imported in BEAUTI, where they were assigned separate and unlinked substitution and clock models. Bayesian analyses were run with uncorrelated lognormal relaxed clocks, birth-death tree prior and three fossil constraints defined by using lognormal statistical distributions. We used the fossil constraints proposed by Aghova et al. (2019) within the genus *Acomys*, and hence the same specifications of lognormal priors: offset of 8.5 Ma for the most recent common ancestor (MRCA) of the genus *Acomys*, 6.08 Ma for the MRCA of the clade encompassing *cahirinus* + *wilsoni* + *russatus* and 3 Ma for the MRCA of the *spinosissimus* group (Aghová et al., 2019); mean = 1 in the three cases (Aghová et al., 2019). Two independent runs were carried out for 50 million generations with sampling every 1000 generations in BEAST. The first 10% were discarded as burn-in and the resulting parameter and tree files were examined for convergence and effective sample sizes in Tracer 1.7 (Rambaut et al., 2018). The two runs were combined in LogCombiner and the species tree was visualized in TreeAnotator.

Morphometrics analyses

First upper molars (UM1) were photographed using a Leica MZ 9.5 binocular, being manually oriented so that the occlusal surface matched at best the horizontal plane. The shape of the UM1 was described using 64 points sampled at equal curvilinear distance along the 2D outline of the occlusal surface using the Optimas software. An outline-based method was chosen, because reliable landmarks are difficult to position on murine-like molars. The top of the cusps is abraded by wear and cannot be used for assessing the position of the cusps, and landmarks bracketing the cusps on

the outline are difficult to position, given the smooth undulations delineating the cusps along the outline. The starting point was tentatively positioned at the anterior-most part of the tooth.

The points along the outline were analysed as sliding semi-landmarks (Cucchi et al., 2013). Using this approach, the outline points are adjusted using a generalized Procrustes superimposition (GPA) standardizing size, position and orientation, while retaining the geometric relationships between specimens (Rohlf & Slice, 1990). During the superimposition, semi-landmarks were allowed sliding along their tangent vectors until their positions minimized the shape difference between specimens, the criterion being bending energy (Bookstein, 1997). Because the first point was only defined on the basis of a maximum of curvature at the anterior-most part of the UM1, some slight offset might occur between specimens. The first point was therefore considered as a semi-landmark allowed to slide between the last and second points.

The centroid size (CS) of the 64 points (i.e. square root of the sum of the squared distance from each point to the centroid of the configuration) was considered as an estimate of overall tooth size. Differences between groups were tested using an analysis of variance (ANOVA) and relationships between variables were assessed using Pearson's product-moment correlation. The pattern of tooth shape differentiation was explored using multivariate analyses of the aligned coordinates. A principal component analysis (PCA on the variance-covariance matrix of the aligned coordinates) allowed a first exploration of the dataset. It was complemented by a between-group PCA (bgPCA). While the PCA is an eigenanalysis of the total variance-covariance of the dataset, the bgPCA analyses the variance-covariance between group means weighted by the sample size of each group.

Size-related variations in shape and differences between groups were investigated using Procrustes ANOVA. With this approach, the Procrustes distances among specimens are used to quantify the components of shape variation, which are statistically evaluated via permutation (here, 9999 permutations) (Adams & Otarola-Castillo, 2013). The allometric relationship was visualized as the common allometric component (CAC) (Adams et al., 2013). To assess the impact of allometry on the pattern of shape differentiation, a bgPCA was also performed on the residuals of a regression of the aligned coordinates vs. centroid size.

The GPA and the Procrustes ANOVA were performed using the R package *geomorph* (Adams & Otarola-Castillo, 2013). The PCA and the bgPCA were performed using the package *ade4* (Dray & Dufour, 2007). For ANOVA and Procrustes ANOVA, the grouping factor was considered to be the region (see Table 1), in order to increase sample size and ameliorate the performance of the tests. For the bgPCA, the grouping factor was the trapping locality. It corresponds to field data, and the

clustering of neighbouring localities in the morphospace is indicative of geographic structure, despite low sample size for small groups.

Results

Genetic analyses

As the phylogenetic trees reconstructed with MrBayes and PhyMl were congruent, only the Bayesian tree is presented (Fig. 2). Two main lineages were found with good support (BP > 0.75, PP > 0.45) within *A. cahirinus s.l.*. Lineage A [according the terminology of (Barome et al., 2001)] consisted of haplotypes from Western and Central Crete, Cyprus, Cairo (Northern Egypt) and Chad. Lineage B involved samples from Eastern and Central Crete, Cilicia, Southern Egypt and Libya. The sequences of Chad and Libya appear to be basal with regards to the two lineages, and they were attributed neither to lineage A nor to B.

Both D-loop and cytochrome b showed two lineages within *A. cahirinus s.l.* and the two mitochondrial genes provided congruent outcomes at the individual level [(Barome et al., 2001; Frynta et al., 2010); this study]. One exception regarded the specimen R155 from Piskopiano (Crete) published with a cyt b sequence belonging to lineage B (Giagia-Athanasopoulou et al., 2011) and for which we found a D-loop belonging to lineage A. We re-sequenced both genes and confirmed the D-loop attribution to lineage A. Another discrepancy regarded the North African specimens, which were attributed to lineage B for the cyt b (Frynta et al., 2010). Based on the present D-loop results, they rather appear to have a basal position in the phylogenetic tree with regards to lineages A and B.

Eastern and Central Crete shared haplotypes with Cilicia. Western and Central Crete shared other haplotypes with Cyprus; none were in common between Cyprus and Cilicia (Fig. 2). This result is confirmed by the Fst being lower between Cyprus and Crete (Fst = 0.28, p = 0.01) and between Cilicia and Crete (Fst = 0.60, P < 0.001) than between Cyprus and Cilicia (Fst = 0.83, P < 0.001). Haplotype diversity was found to be higher in Crete (Hd = 0.864) than in Cyprus (Hd = 0.667) or Cilicia (Hd = 0.448).

In the network (Fig. 3), a finer geographic structure could be recognized, especially in Crete. The few African samples appeared as central in the network, with the exception of Cairo, which appeared to be divergent but nested within lineage A. Haplotypes from Crete appeared intermediate between the basal African haplotypes and either those of Cyprus (for lineage A) or those of Cilicia (for lineage B). A geographic structure emerged in Crete, with different haplotypes found in the West, Centre and East of the island. Within lineage A, a central haplotype (in blue on Fig. 3) was found in both Western

Crete and in Cyprus; other haplotypes were either characteristics of Western or Central Crete. Eastern Crete was characterized by a haplotype affiliated to lineage B, also present in the easternmost locality of Central Crete (Stalida Mochos) and in Cilicia. Cilicia further hosted two specific haplotypes, while Cyprus displayed three specific haplotypes.

Based on a combined analysis of mitochondrial (Cyt *b* + D-loop) and nuclear genes (IRBP, RAG1), the divergence between the two lineages was estimated at 210 000 years [110 000 - 320 000] (Supp. Figure 1).

Morphometric analysis of the first upper molar differentiation

Sexual dimorphism

Data on sex and body size (head + body length) were available for most specimens. Body size, as well as UM1 centroid size, were well differentiated among regions, but not between sexes (Table 2). Tooth shape was also very different among regions, while sexes were only weakly differentiated. As a consequence, males and females were pooled in subsequent analyses, to focus on geographical patterns of differentiation.

Geographic variations in size and relationship between body and tooth size

Body size varied greatly among but also within populations (Fig. 4A). This variation is partly due to the age structure of the populations, since very young animals can be trapped, as shown by the specimen without erupted third molars, which displays a very small body size. Specimens from Western Crete tended to display the largest body size, whereas those from Cilicia were among the smallest. Animals from Cyprus and Cairo tended to have a large body size.

This trend was not reflected in the pattern of molar size variation (Fig. 4B). Animals from Western Crete, while being among the largest, displayed small molar teeth. Similarly, the large animals from Cairo displayed extremely small teeth, while the spiny mice from Cyprus, of similar body size, displayed among the largest teeth of the dataset. As a consequence, body and molar size were not related (Fig. 4C). In a model including region and body size as explanatory variables, UM1 centroid size varied greatly among regions ($P < 2e\text{-}16$) but only weakly with body size ($P = 0.0158$).

Overall, tooth size displayed a reduced variation within localities and within regions, in contrast to body size, but the differences in molar size were important even among regions of Crete. Spiny mice from Saharan regions (Sudan and Chad) displayed important variations in molar size, even within

Sudan, despite the fact that these mice were all derived from Khartoum. The fossil teeth from Kommos were of large size, similar to the modern Central and Eastern Cretan populations.

Tooth shape differences among populations

The different regions were highly different in shape (Procrustes ANOVA: $P < 0.0001$). In the morphospace defined by the first two axes of the PCA on the aligned coordinates (Fig. 5A), populations from Western and Eastern Crete were opposed along PC1. This axis describes a change from teeth with receding anterior cusps leading to an elongated anterior part, to teeth with prominent, anteriorly shifted lingual cusp t1 and labial cusp t3 (Fig. 5B). Negative scores along PC2 characterize teeth from Cyprus, with a broader and rounder posterior part, closer labial cusps (t3 and t9), an anteriorly shifted lingual cusp t1, and an anterior part compressed on the lingual side (Fig. 5C).

A bgPCA (Fig. 5D) provided further insight into the geographic clustering on Crete. The populations of Western Crete appeared as the most differentiated. The Central and Eastern Cretan populations were relatively close to each other. The Cilician populations appeared central in this morphospace. Along the second axis of the bgPCA, Cyprus appeared as highly divergent. At the opposite side of this axis, the two African samples shared high positive scores; the sample from Cairo was closer to Western Crete along bgPC1, whereas the Saharan sample was closer to Central and Eastern Crete. The populations from Central Crete varied along bgPC2, the two samples from Piskopiano and surroundings displaying positive bgPC2 scores, whereas the three other localities shared negative bgPC2 scores. The fossil teeth from Kommos plotted close to the samples from Sahara and Piskopiano in Central Crete.

Allometric tooth shape variation

Since tooth size variation appeared to be important (Fig. 4), allometry was investigated as a source of shape differentiation. Shape appeared as significantly related to size (Procrustes ANOVA: $p = 1e\text{-}04$). The Common Allometric Component (CAC) based on this analysis (Fig. 6A) showed a general size-shape trend which may contribute to the shape similarity between the populations with small molars (Cairo, Western Crete) and to those sharing large molar size (Eastern Crete and Cyprus). Large teeth tended to display a prominent and anteriorly shifted first lingual cusp (t1) and a prominent posterior labial cusp (t9) compared to small teeth (Fig. 6B).

The size-free shape variation was explored based on a bgPCA on the residuals of a regression of the aligned coordinates on centroid size (Fig. 6C). The pattern of between-population differentiation was not deeply modified compared to the analysis on the raw aligned coordinates (Fig. 5D).

Discussion

Two ancient haplogroups in Crete

This study confirms the complex geographic structure observed in earlier studies within the Eastern Mediterranean spiny mice *Acomys cahirinus s.l.* (Barome et al., 2001; Frynta et al., 2010; Giagia-Athanasopoulou et al., 2011). Different haplogroups occur in Cyprus and Cilicia, the only area where *Acomys cahirinus s.l.* occurs on a Northern Mediterranean coast, while Crete hosts both haplogroups (Barome et al., 2001; Frynta et al., 2010). The divergence of the two haplogroups has been dated here at 210 kyrs, an estimate based on four genes, several calibration points within *Acomys*, and a Bayesian approach, that allows to re-evaluate the previous estimate of 400 kyrs (Barome et al., 2001). Such a range of dating of divergence is typical for phylogeographic lineages isolated during the Plio-Pleistocene climatic fluctuations [e.g. (Nicolas et al., 2008; Ben Faleh et al., 2012; McDonough et al., 2015)]. Since a Pleistocene fossil record of *Acomys* is absent from Cyprus and Crete (Barome et al., 2001), the divergence between the haplogroups clearly predates the dispersion in this area.

A complex geographic structure in Cretan spiny mice

The two mitochondrial lineages have different geographic distributions: lineage A dominates in Western and Central Crete, whereas lineage B occurs mostly in Eastern Crete (Barome et al., 2001; Frynta et al., 2010; Giagia-Athanasopoulou et al., 2011). The present study further shows a finer geographic structure, based on the repartition of the D-loop haplotypes: Western and Central Crete tend to display different haplotypes within lineage A (Fig. 3). This is in complete agreement with the morphometric results, showing different molar size (Fig. 4) and shape (Fig. 5) in Western, Central and Eastern Crete; possibly, a finer differentiation occurs even within Central Crete, with the area around Piskopiano displaying slightly different molar shape (Fig. 5). A reconsideration of the former chromosomal results (Giagia-Athanasopoulou et al., 2011) also suggests regional variations in Crete (Fig. 7), with high, ancestral, diploid chromosome numbers (up to $2n = 42$) dominating in Central Crete, whereas lower, derived diploid chromosome numbers (e.g. $2n = 38$) are found in Western and Eastern Crete (Fig. 7). All markers, despite being very different in their nature (mitochondrial DNA,

326 karyotypes, molar size and shape) are therefore congruent and point to a strong geographic
327 structure in Crete.

328 Nevertheless, evidence of mixing occurs. Regarding the mitochondrial lineages, specimens attributed
329 to lineage B can occasionally be found in regions dominated by lineage A: one mouse in Akrotiri
330 Peninsula, Chania (Barome et al., 2001) and one mouse in the easternmost locality of Central Crete,
331 Stalida Mochos [(Giagia-Athanasopoulou et al., 2011); this study]. Regarding karyotypes, a specimen
332 with the derived diploid chromosome number 2*n* = 38 was found in Central Crete, despite the
333 dominance there of high diploid chromosome numbers (2*n* = 42, 2*n* = 40 and their hybrids). The
334 occurrence in Eastern Crete of both, homozygous mice with 2*n* = 40 and heterozygotes with 2*n* = 39
335 suggests the existence in the area of homozygous mice with *2n* = 38, although they have not yet
336 been captured [Fig. 7, (Giagia-Athanasopoulou et al., 2011)].

337 Despite this evidence of mixing, the strong geographic structure observed for molar shape shows
338 that gene flow is not enough to homogenize the populations across Crete. Crete is characterized by a
339 mountainous relief compartmented by basins, with several massifs culminating above 2000 meters.
340 Both high mountains and basins may constitute barriers to dispersal for spiny mice preferably
341 inhabiting Mediterranean environments with rocky substrates (Kryštufek & Vohralík, 2009). This
342 complex geomorphology probably promoted isolation and divergence of *Acomys* populations in
343 different parts of the island.

344

345 *Cretan spiny mice within the diversity of the Eastern Mediterranean area*

346 The diversity observed in Cretan spiny mice is difficult to insert into a general pattern, because the
347 diversity on the African continent is largely under-sampled. However, the distribution of the two
348 haplogroups in the Eastern Mediterranean area points to a complex history of migration. The
349 haplotypes found in Crete, Cyprus and Cilicia were shown to be derived, compared to the haplotypes
350 sampled so far in Libya, Chad, and the high Nile Valley. Chadian and Libyan specimens even appeared
351 to be outside from lineage A or B, due to their basal position, or to incomplete lineage sorting. In
352 contrast, lineage A haplotypes sampled in Cairo appeared to be derived and branched with
353 sequences from Cyprus and Western Crete [(Frynta et al., 2010); this study].

354 Regarding the karyotype evolution, *Acomys* is characterized by an important variation of the diploid
355 chromosome number, ranging from 2*n* = 68 to 2*n* = 40-42 and even 2*n* = 38-36 in the *A. cahirinus*
356 group, knowing that 2*n* = 36 is the karyotype with the lowest chromosome number that can be
357 achieved in spiny mice through Rb fusions (Lavrenchenko et al., 2011). Within *A. cahirinus*, 2*n*=40-42

karyotypes can therefore be considered as 'ancestral' and those of 2*n* = 36-38 as 'derived'. In particular, Central Crete hosts ancestral karyotypes (2*n* = 40 and even 2*n* = 42). Cyprus displays an additional Robertsonian (Rb) fusion (2*n* = 38), that is also present in Western Crete and possibly in Eastern Crete. A further Rb fusion has led to 2*n* = 36 in the Cilicia population and in the Egyptian population from Cairo (Macholán et al., 1995; Zima et al., 1999; Giagia-Athanasopoulou et al., 2011). However, it is difficult to assess the variation within *A. cahirinus* in the African continent, due to a limited geographic sampling and taxonomic uncertainty.

Regarding molar morphometrics, the population from Central Crete appears close to the Saharan group and to the fossil teeth from Kommos. Altogether, this suggests that Central Crete may host a population characterized by ancestral tooth morphology, karyotypes, and haplotypes. The Cretan fossils were deposited during the lifetime of the Hellenistic temple of Kommos, which lasted from 375 BC to AD 160/170. Since no *Acomys* fossils were ever found in older Cretan deposits (Katerina Papayiannis pers. obs. January 2020), this places the earliest appearance of *Acomys* on Crete during this time interval.

The occurrence of a second mitochondrial lineage in Eastern Crete (lineage B), however, suggests that multiple introductions occurred from different continental source populations. Important trade across the Eastern Mediterranean area continued throughout the Bronze Age and Historic times (Karetsou et al., 2001). Likely, the dispersion of *Acomys* through the Eastern Mediterranean area occurred by human-mediated transport (Barome et al., 2001) as unintentional stowaway on boat cargos, in a manner similar to that described for the Western house mouse *Mus musculus domesticus* (Cucchi, 2008). Both Cilicia and Cyprus spiny mice display more derived haplotypes, karyotypes, and tooth shape than those from Crete; this further suggests that Crete acted as a hub from which spiny mice were translocated.

In support of this statement, the fact that the 2*n* = 38 karyotype of some Cretan spiny mice is identical to the one of Cypriot mice, and differs only by an additional Rb fusion from the 2n = 36 karyotype of Cilician mice, could be explained through the expansion of mice with 2*n* = 38 from Crete to the other two regions, irrespective of mitochondrial lineages. The two lineages are reported to freely hybridize in the laboratory (Frynta et al., 2010) and in Crete, they are not associated with specific karyotypes, e.g. there exist spiny mice with 2*n* = 38 attributed to lineage A or B (Giagia-Athanasopoulou et al., 2011). Thus, populations with 2*n* = 38 could have been imported to Cilicia from Eastern Crete (dominated by lineage B) and to Cyprus from Central or Western Crete (dominated by lineage A). The additional Rb fusion, mentioned above, would have then occurred locally in the isolated population of Cilicia, leading to its very derived karyotype (2*n* = 36).

The population from Cairo constitutes a puzzling case. It displays the same derived karyotype as Cilicia (2*n* = 36 with the same Rb fusions), however belongs to lineage A, with haplotypes related to those of Cyprus and Western Crete. Thus, a direct relationship between the Cairo and Cilician spiny mice is unlikely. Moreover, the tooth morphology of the Cairo mice is close in size and shape to the one observed in Western Crete. These facts could be reconciled if the population from Cairo is actually derived from a secondary import on the African continent, from Western Crete or Cyprus.

In this case, the identical karyotype of 2*n* = 36 in both Cilicia and Cairo would be the result of the independent, *in situ* fixation of the same Rb fusion in the karyotype of both populations. Derived from 2*n* = 38, there are only three acrocentric chromosomes available for a new Rb fusion, one of which is very small (Giagia-Athanasopoulou et al., 2011). Rb fusions do not happen completely randomly between acrocentric chromosomes, but similarly-sized chromosomes seem to be preferably fused (Gazave et al., 2003), and this may have triggered the independent fixation of the same Rb fusion in the two, otherwise, distant populations (Lavrenchenko et al., 2011). As in the house mouse, successive Rb fusions, leading to very low diploid numbers, might have been favoured by successive dispersion events, and small patchy distribution (Auffray, 1993). The peculiarity of the Cairo population could be maintained by behavioural mechanisms, similar to those reported for house mouse populations from Tunisia (Chatti et al., 1999), since this population is characterized by its commensal habit (Kryštufek & Vohralík, 2009) that may maintain its isolation from the surrounding populations. Any further interpretation is hampered by the limited data available from the African continent.

Insularity and isolation promoting morphological divergence

Whatever the dynamics of colonization, the insular conditions promoted a pronounced morphological divergence in tooth morphology. This occurred in a relatively short evolutionary time span, since the first appearance of *Acomys* in Crete occurred during the Hellenistic period, ~2000 years ago (Payne, 1995). The evolution on Cyprus is even more rapid. Since no *Acomys* fossil has been recovered so far from the prehistoric record (Vigne, 1999; Horwitz et al., 2004), the species is thought to have been introduced to this island during the last 1000 years. In that time span, the molar morphology evolved markedly, exemplifying the acceleration of morphological evolution on islands (Millien, 2006). Morphological divergence occurred as well in the isolated but not insular population of Cilicia, although to a lesser degree. This suggests that random drift in isolated, small populations fostered rapid divergence in Crete, Cyprus and Cilicia, and that adaptation to local insular conditions has further drove molar evolution in the two insular populations, as shown for the house

mouse (Ledevin et al., 2016). In addition, hybridization between the populations of Crete might have contributed to the diversity of molar shape on this island. Hybrid morphologies are not necessarily intermediate between those of the parents, but can display transgressive phenotypes (Renaud et al., 2017a). In Central Crete, molars frequently display an elongated forepart up to the occurrence of a small, additional cusplet in front of the t2 cusp. A similar phenotype was found in hybrid house mice (Renaud et al., 2017a), and in several insular house mouse populations (Renaud et al., 2011; Renaud et al., 2018). The evolution of similar dental phenotypes in distant rodent groups might be due to shared developmental processes favouring not only convergent evolution within true murines (Hayden et al., 2020), but also between murines and the murine-like molar of *Acomys*.

Heterogeneity in molar size: a partial decoupling from body size

Evolution of size is a well-known characteristic of insular populations (Lomolino, 1985, 2005). Small mammals are expected to increase in body size, due to a combination of factors including decrease of interspecific competition and predation pressure, and increase of intraspecific competition (Lomolino, 1985, 2005). Because molar size is considered to be a good proxy of body size at a broad taxonomic scale (Gingerich et al., 1982), increase in molar size could be expected as well.

Regarding body size, *Acomys* indeed displayed a large body size on Cyprus, but within Crete, body size varied considerably among populations (Fig. 4A). This may be related to different age structure of the populations: sampling at different periods may lead to an overrepresentation of young or old animals, skewing the size distribution towards small or large body size (Renaud et al., 2017b). Such a confounding factor may be especially important in a species in which neonates already display hair and open eyes, and can therefore rapidly leave the nest. Age structure may also contribute to the large body size observed for most specimens from Cairo, that are mentioned to have been maintained in captivity for some time.

Estimating the degree of insular size increase is all the more difficult, due to the lack of sufficient data for African spiny mice. Nevertheless, among Eastern Mediterranean spiny mice, the continental Cilician *Acomys* displayed the smallest body size. Differences between Cypriot and Cretan mice may be related to local differences in competition and predation. For instance, the least weasel (*Mustela nivalis*) has been intentionally introduced by Phoenicians and Greeks on the Mediterranean islands, with the aim of controlling commensal rodents following their stowaway introduction (Rodrigues et al., 2017). The weasels introduced in antiquity (Lehmann & Nobis, 1979), however went extinct in Cyprus (Rodrigues et al., 2017), further relieving mammalian predation pressure on Cypriot *Acomys*.

In contrast, molar size varied greatly among Crete, Cyprus and Cilicia, and even within Crete. This apparently surprising uncoupling between molar and body size is due to the fact that even if molar size is correlated to body size at a broad taxonomic scale, it is not necessarily the case at a population level, because the first molar erupts early after birth and is therefore not affected by subsequent growth (Renaud et al., 2017b). The most obvious decoupling between body and molar size regards the populations from Western Crete and Cairo, being of relatively large body size but extremely small molar size (Fig. 4C). Similar uncoupling is not uncommon and has been observed for instance in wood mice (*Apodemus sylvaticus*) from Ibiza (Renaud & Michaux, 2007).

The large variation in molar size may echo an under-evaluated variation in the African continent, as suggested by the large variation in tooth size observed in Khartoum, Sudan (Fig. 4B). It could also have an adaptive component, for instance related to a polarity in rainfall in Crete, western regions receiving more rainfall and thus hosting different ecosystems. Indeed, larger tooth size ("macrodonty") has been proposed to occur in some insular small mammals, as a response to diet shifts (Vigne et al., 1993). Large teeth with a massive outline, as those of Eastern Crete, might be favoured in dry habitats, in order to process more efficiently hard food, resistant to comminution (Renaud et al., 2005).

Conclusion

Genetic, chromosomal and morphometric results were congruent to underline a strong geographic structure in Eastern Mediterranean spiny mice (*Acomys cahirinus* sensu lato) and especially within Crete. A complex history of multiple introductions is probably responsible for this structure. Insular isolation coupled with habitat shift must have further promoted a pronounced and rapid morphological evolution in molar size and shape on Crete and Cyprus.

As a consequence, the species *A. nesiotes* (Cyprus), *A. cilicicus* (Cilicia, Turkey) and *A. minous* (Crete) are clearly nested within *A. cahirinus* (group cah9 in (Aghová et al., 2019)) and are only defined by their geographic distribution. Due to their isolated distribution and morphological characteristics, "*nesiotes*" and "*cilicicus*" names may be maintained for describing subspecific evolutionary units. *A. minous* encompasses populations with different haplotypic composition and morphometric characteristics, and therefore it does not correspond to a homogeneous evolutionary unit. A more thorough sampling of the African continent, as well as further genetic data including nuclear genes, would be required for a better understanding of the complex history of translocation and evolution in isolation that led to the amazing morphological diversity in modern Cretan and more generally, Eastern Mediterranean spiny mice.

Acknowledgements

We thank the three anonymous reviewers for their constructive comments. The sampling in Turkey benefited from a funding by the Zonguldak Bulent Ecevit University project (no 2012-10-06-10) to Mustafa Sözen and Ferhat Matur.

References

Adams CD, Otarola-Castillo E. 2013. geomorph: an R package for the collection and analysis of geometric morphometric shape data. *Methods in Ecology and Evolution* **4:** 393-399.

Adams CD, Rohlf FJ, Slice DE. 2013. A field comes of age: geometric morphometrics in the 21th century. *Hystrix, The Italian Journal of Mammalogy* **24:** 7-14.

Aghová T, Palupčíková K, Šumbera R, Frynta D, Lavrenchenko LA, Meheretu Y, Sádlová J, Votýpka J, Mbau JS, Modrý D, Bryja J. 2019. Multiple radiations of spiny mice (Rodentia: *Acomys*) in dry open habitats of Afro-Arabia: evidence from a multi-locus phylogeny. *BMC Evolutionary Biology* **19:** 69.

Auffray J-C. 1993. Chromosomal divergence in house mice in the light of palaeonotlogy: a colonization-related event? *Quaternary International* **19:** 21-25.

Barome P-O, Lymberakis P, Monnerot M, Gautun J-C. 2001. Cytochrome *b* sequences reveal *Acomys minous* (Rodentia, Muridae) paraphyly and answer the question about the ancestral karyotype of *Acomys dimidiatus*. *Molecular Phylogenetics and Evolution* **18:** 37-46.

Ben Faleh A, Granjon L, Tatard C, Boratyński Z, Cosson J-F, Said K. 2012. Phylogeography of two cryptic species of African desert jerboas (Dipodidae: *Jaculus*). *Biological Journal of the Linnean Society* **107:** 27-38.

Bookstein FL. 1997. Landmark methods for forms without landmarks: morphometrics of group differences in outline shape. *Medical Image Analysis* **1:** 225-243.

Bouckaert R, Vaughan TG, Barido-Sottani J, Duchêne S, Fourment M, Gavryushkina A, Heled J, Jones G, Kühnert D, De Maio N, Matschiner M, Mendes FK, Müller NF, Ogilvie HA, du Plessis L, Popinga A, Rambaut A, Rasmussen D, Siveroni I, Suchard MA, Wu CH, Xie D, Zhang C, Stadler T, Drummond AJ. 2019. BEAST 2.5: An advanced software platform for Bayesian evolutionary analysis. *PLoS Computional Biology* **15:** e1006650.

Caumul R, Polly PD. 2005. Phylogenetic and environmental components of morphological variation: skull, mandible, and molar shape in marmots (*Marmota*, Rodentia). *Evolution* **59:** 2460-2472.

Chatti N, Ganem G, Benzekri C, Catalan J, Britton-Davidian J, Saïd K. 1999. Microgeographical distribution of two chromosomal races of house mice in Tunisia: pattern and origin of habitat partitioning. *Proceedings of the Royal Society of London, Biological Sciences (serie B)* **266:** 1561-1569.

Cucchi T. 2008. Uluburun shipwreck stowaway house mouse: molar shape analysis and indirect clues about the vessel's last journey. *Journal of Archaeological Science* **35:** 2953-2959.

Cucchi T, Kovács ZE, Berthon R, Orth A, Bonhomme F, Evin A, Siahsarvie R, Darvish J, Bakhshaliyev V, Marro C. 2013. On the trail of Neolithic mice and men towards Transcaucasia: zooarchaeological clues from Nakhchivan (Azerbaijan). *Biological Journal of the Linnean Society* **108:** 917-928.

Darriba D, Taboada GL, Doallo R, Posada D. 2012. jModelTest 2: more models, new heuristics and parallel computing. *Nature Methods* **9:** 772.

Denys C, Gautun J-C, Tranier M, Volobouev V. 1994. Evolution of the genus *Acomys* (Rodentia, Muridae) from dental and chromosomal pattern. *Israel Journal of Zoology* **40:** 215-246.

Dray S, Dufour A-B. 2007. The ade4 package: implementing the duality diagram for ecologists. *Journal of Statistical Software* **22:** 1-20.

Frynta D, Palupčíkova K, Bellinvia E, Benda P, Skarlantová H, Schwarzová L, Modry D. 2010. Phylogenetic relationships within the *cahirinus-dimidiatus* group of the genus *Acomys* (Rodentia: Muridae): a new mitochondrial lineage from Sahara, Iran and the Arabian Peninsula. *Zootaxa* **2660:** 46-56.

Gazave E, Catalan J, Da Graça Ramalhinho M, Da Luz Mathias M, Nunes M, Dumas D, Britton-Davidian J, Auffray J-C. 2003. The non-random occurrence of Robertsonian fusionin the house mouse. *Genetical Research* **81:** 33-42.

Giagia-Athanasopoulou EB, Rovatsos MT, Mitsainas GP, Martimianakis S, Lymberakis P, Angelou L-XD, Marchal JA, Sánchez A. 2011. New data on the evolution of the Cretan spiny mouse, *Acomys minous* (Rodentia, Murinae), shed light on the phylogenetic relationships in the *cahirinus* group. *Biological Journal of the Linnean Society* **102:** 498-509.

Gingerich PD, Smith BH, Rosenberg K. 1982. Allometric scaling in the dentition of primates and prediction of body weight from tooth size in fossils. *American Journal of Physical Anthropology* **58:** 81-100.

Gouy M, Guindon S, Gascuel O. 2010. SeaView Version 4: A multiplatform graphical user interface for sequence alignment and phylogenetic tree building. *Molecular Biology and Evolution* **27:** 221-224.

Guindon S, Dufayard J-F, Lefort V, Anisimova M, Hordijk W, Gascuel O. 2010. New algorithms and methods to estimate maximum-likelihood phylogenies: assessing the performance of PhyML 3.0. *Systematic Biology* **59:** 307-321.

Hayden L, Lochovska L, Sémon M, Renaud S, Delignette-Muller M-L, Vicot M, Peterková R, Hovorakova M, Pantalacci S. 2020. Developmental variability channels mouse molar evolution. *eLife* **9:** e50103.

Horwitz LK, Tchernov E, Hongo H. 2004. The domestic status of the early Neolithic fauna of Cyprus: a view from the mainland. In: Peltenburg E and Wasse A, eds. *Neolithic revolution: new perspectives on Southwest Asia in light of recent discoveries on Cyprus*. Oxford: Oxbow books. 135-148.

Karetsou A, Andreadaki-Vlasaki M, Papadakis N. 2001. Crete-Egypt: three thousand years of cultural links, Catalogue. In: Hellenic Ministry of Culture DoPaCA, ed.

Kryštufek B, Vohralík V. 2009. Mammals of Turkey and Cyprus. Rodentia II: Cricetinae, Muridae, Spalacidae, Calomyscidae, Capromyidae, Hystricidae, Castoridae. In: Kryštufek B and Vohralík V, eds. *Mammals of Turkey and Cyprus.* Univerza na Primorskem: Koper.

Lanfear R, Frandsen PB, Wright AM, Senfeld T, Calcott B. 2017. Partitionfinder 2: New methods for selecting partitioned models of evolution for molecular and morphological phylogenetic analyses. *Molecular Biology and Evolution* **34:** 772-773.

Lavrenchenko LA, Nadjafova RS, Bulatova NS. 2011. Three new karyotypes extend a Robertsonian fan in Ethiopian spiny mice of the genus *Acomys* I. Geoffroy, 1838 (Mammalia, Rodentia). *Comparative Cytogenetics* **5:** 423-431.

Ledevin R, Chevret P, Ganem G, Britton-Davidian J, Hardouin EA, Chapuis J-L, Pisanu B, Mathias MdL, Schlager S, Auffray J-C, Renaud S. 2016. Phylogeny and adaptation shape the teeth of insular mice. *Proceedings of the Royal Society of London, Biological Sciences (serie B)* **283:** 20152820.

Ledevin R, Quéré J-P, Michaux JR, Renaud S. 2012. Can tooth differentiation help to understand species coexistence? The case of wood mice in China. *Journal of Zoological Systematics and Evolutionary Research* **50:** 315-327.

Librado P, Rozas J. 2009. DnaSP v5: a software for comprehensive analysis of DNA polymorphism data. *Bioinformatics* **25:** 1451-1452.

584 **Lomolino MV. 1985.** Body size of mammals on islands: the island rule reexamined. *The American*
585 *Naturalist* **125:** 310-316.
586 **Lomolino MV. 2005.** Body size evolution in insular vertebrates: generality of the island rule. *Journal*
587 *of Biogeography* **32:** 1683-1699.
588 **Macholán M, Zima J, Cervená A, Cervený J. 1995.** Karyotype of *Acomys cilicicus* Spitzenberger, 1978
589 (Rodentia, Muridae). *Mammalia* **59:** 397-402.
590 **McDonough MM, Šumbera R, Mazoch V, Ferguson AW, Phillips CD, Bryja J. 2015.** Multilocus
591 phylogeography of a widespread savanna–woodland-adapted rodent reveals the influence of
592 Pleistocene geomorphology and climate change in Africa's Zambezi region. *Molecular*
593 *Ecology* **24:** 5248–5266.
594 **Millien V. 2006.** Morphological evolution is accelerated among island mammals. *PLoS Biology* **4:**
595 e321.
596 **Nicolas V, Bryja J, Akpatou B, Konecny A, Lecompte E, Colyn M, Lalis A, Couloux A, Denys C,**
597 **Granjon L. 2008.** Comparative phylogeography of two sibling species of forest-dwelling
598 rodent (*Praomys rostratus* and *P. tullbergi*) in West Africa: different reactions to past forest
599 fragmentation. *Molecular Ecology* **17:** 5118-5134.
600 **Nicolas V, Granjon L, Duplantier J, Cruaud C, Dobigny G. 2009.** Phylogeography of spiny mice (genus
601 *Acomys*, Rodentia: Muridae) from the south-western margin of the Sahara with taxonomic
602 implications. *Biological Journal of the Linnean Society* **98:** 29-46.
603 **Payne S. 1995.** Appendix 5.1: The small mammals. In: Shaw JW and Shaw M, eds. *The Kommos region*
604 *and the houses of the Minoan town. Part 1: the Kommos region, ecology and Minoan*
605 *industries.* Princeton: Princeton University Press. 278-291.
606 **Rambaut A. 2012.** Figtree v1.4. http://tree.bio.ed.ac.uk/software/figtree/.
607 **Rambaut A, Drummond AJ, Xie D, Baele G, Suchard MA. 2018.** Posterior summarisation in Bayesian
608 phylogenetics using Tracer 1.7. *Systematic Biology* **67:** syy032.
609 **Renaud S, Alibert P, Auffray J-C. 2017a.** Impact of hybridization on shape, variation and covariation
610 of the mouse molar. *Evolutionary Biology* **44:** 69-81.
611 **Renaud S, Hardouin EA, Quéré J-P, Chevret P. 2017b.** Morphometric variations at an ecological
612 scale: Seasonal and local variations in feral and commensal house mice. *Mammalian Biology*
613 **87:** 1-12.
614 **Renaud S, Ledevin R, Souquet L, Gomes Rodrigues H, Ginot S, Agret S, Claude J, Herrel A, Hautier L.**
615 **2018.** Evolving teeth within a stable masticatory apparatus in Orkney mice. *Evolutionary*
616 *Biology* **45:** 405-424.
617 **Renaud S, Michaux J, Schmidt DN, Aguilar J-P, Mein P, Auffray J-C. 2005.** Morphological evolution,
618 ecological diversification and climate change in rodents. *Proceedings of the Royal Society of*
619 *London, Biological Sciences (serie B)* **272:** 609-617.
620 **Renaud S, Michaux JR. 2007.** Mandibles and molars of the wood mouse, *Apodemus sylvaticus* (L.):
621 integrated latitudinal signal and mosaic insular evolution. *Journal of Biogeography* **34:** 339-
622 355.
623 **Renaud S, Pantalacci S, Auffray J-C. 2011.** Differential evolvability along lines of least resistance of
624 upper and lower molars in island house mice. *PLoS ONE* **6:** e18951.
625 **Rodrigues M, Bos AR, Schembri PJ, Lima RFd, Lymberakis P, Parpal L, Cento M, Ruette S, Ozkurt SO,**
626 **Santos-Reis M, Merilä J, Fernandes C. 2017.** Origin and introduction history of the least
627 weasel (*Mustela nivalis*) on Mediterranean and Atlantic islands inferred from genetic data.
628 *Biological Invasions* **19**.
629 **Rohlf FJ, Slice D. 1990.** Extensions of the Procrustes method for the optimal superimposition of
630 landmarks. *Systematic Zoology* **39:** 40-59.
631 **Ronquist F, Teslenko M, Mark Pvd, Ayres D, Darling A, Höhna S, Larget B, Liu L, Suchard MA,**
632 **Huelsenbeck JP. 2012.** MrBayes 3.2: Efficient Bayesian phylogenetic inference and model
633 choice across a large model space. *Systematic Biology* **61:** 539-542.

Shaw JW. 2000. Chapter 1: the architecture of the Temples and other buildings. In: Shaw JW and Shaw MC, eds. *Kommos IV: the Greek Sanctuary, part 1.* Princeton: Princeton University Press. 37-56.

Vigne J-D. 1999. The large 'true' Mediterranean islands as a model for the Holocene human impact on the European vertebrate fauna? Recent data and new reflections. In: Benecke N, ed. *The Holocene history of the European vertebrate fauna: modern aspects of research*. Leidorf: Archäologisches Institut Eurasien. 295-322.

Vigne J-D, Cheylan G, Granjon L, Auffray J-C. 1993. Evolution ostéométrique de *Rattus rattus* et de *Mus musculus domesticus* sur de petites îles: comparaison de populations médiévales et actuelles des îles Lavezzi (Corse) et de Corse. *Mammalia* **57:** 85-98.

Volobouev V, Auffray J-C, Debat V, Denys C, Gautun J-C, Tranier M. 2007. Species delimitation in the *Acomys cahirinus-dimidiatus* complex (Rodentia, Muridae) inferred from chromosomal and morphological analyses. *Biological Journal of the Linnean Society* **91:** 203-214.

Zima J, Macholán M, Piálek J, Slivková L, Suchomelová E. 1999. Chromosomal banding pattern in the Cyprus spiny mouse, *Acomys nesiotes*. *Folia Zoologica* **48:** 149-152.

650 **Tables**

651

Area	Region	Locality	Code	N UM1	N Dloop	New accession numbers
Crete	West (W)	Chania – Akrotirio	CHA	5	**1**	MT001851
		Lefka Ori	LEFKO	5	**1**	MT001845
		Chania – Souda	SOU	3	**1**	MT001848
		Hills facing Elafonisos island			1	
		Kournas Lake			1	
	Central (C)	Almyros Gorge, Linoperamata	LINO	6	**1**	MT001852
		Kokkini Hani	KOKH	8	**1**	MT001844
		Stalida Mochos	STAL	3	**1**	MT001846
		Piskopiano	PISKO	5	**2**	MT001847 MT043301
		Towards Kokkini Chani	PKOK	20	**1**	MT001853
	East (E)	Siteia	SIT	6	**2**	MT001849 MT001850
		Vai			2	
Cyprus		Cap Greco	CYP	6	**5**	MT001854-58
		Agirdag			1	
		Cinarli			1	
		Zafer Burnu, Cap Andreas			1	
Turkey	Cilicia (CIL)	Narlıkuyu	NAR	8	**6**	MT001830-35
		Ayaş	AYA	4	**3**	MT001836-38
		Karaahmetli, Hüseyinler, Kumrukuyu	KAR	7	**5**	MT001839-43
		Silifke			2	
		NA			1	
Libya		Mts. Akakus			1	
Egypt	Cairo	Cairo	CAIRO	8	2	
	Assouan	Abu Simbel			2	
Sahara	Sahara	Sudan (Kharthoum)	SAH	3		
		Chad (Yogoum)	SAH	1		
		Chad (Tibesti plateau)			1	
Fossil Crete	Central Crete	Kommos	Fos-KOM	3		

652

653 **Table 1.** Sampling for morphometric and genetic analyses. Region, area within region, locality of
654 trapping and its code are provided. N UM1: number of first upper molars included in the analysis. N
655 Dloop: number of Dloop sequences in the present study. In bold the number of newly acquired
656 sequences.

657

658
659

Method	Variable(s)	Region	Sex	Interaction
ANOVA	HBL	**< 0.0001**	0.8050	0.9425
	UM1 CS	**< 0.0001**	0.1679	0.7630
ProcANOVA	UM1 Shape	**< 0.0001**	0.0133	0.0028

Table 2. Sexual dimorphism in molar size and shape, taking into account the regions. Probabilities of ANOVA are given for size univariate parameters (HBL: head + body length; UM1 CS: first upper molar centroid size) and of Procrustes ANOVA for shape data (aligned coordinates).

Figure Captions

Figure 1. Sampling localities and examples of first upper molars (UM1) in the various populations of *Acomys* considered in this study. All belong to the *cahirinus s.l.* group. Spiny mice from the island of Crete are designated as *A. minous*, those from the island of Cyprus as *A. nesiotes* and those confined to a small area in Cilicia (Asia Minor, Turkey) as *A. cilicicus*. Nomenclature of the cusps is indicated on one molar tooth of *A. cilicicus*. The boxes indicate the color code of the areas in figures for morphometrics. For abbreviations of some localities (LINO, STAL, PISKO) see Table 1. All teeth to the same scale (scale bar bottom right).

Figure 2. Bayesian phylogeny of D-loop haplotypes of *Acomys cahirinus s.l.*. Posterior probability and bootstrap support are indicated for each node. " – " indicates that the node is not supported in the phylogeny reconstructed with PhyML.

Figure 3. Network and geographic distribution of the D-loop haplotypes. A. Median-joining haplotype network. B. Geographic repartition of the haplotypes. Each haplotype is identified by the same color code on both figures.

Figure 4. Size variation of *Acomys cahirinus* s.l. A. Body size (Head + Body Length) in the modern populations from Crete, Cyprus, Turkey, Cairo and Sahara. B. Size of the first upper molar (UM1) in the same populations; fossils from Kommos (Iron Age, Crete) are also included. C. Relationship between body and molar size. The Chadian specimen among the Sahara sample is indicated by "Chad" or "C". The arrow with "No UM3" points to a young specimen without erupted third molar.

Figure 5. Shape differentiation of the first upper molar between the different populations of *Acomys cahirinus* s.l., including the fossil teeth from Kommos (Iron Age, Crete). A. Morphospace defined by the first two axes of a PCA on the aligned coordinates of the points delineating the outline of the first upper molar. Each dot corresponds to a tooth. "C" indicates the Chadian specimen in the Sahara sample. B, C: Deformation along the PC axes. Arrows point from the shape corresponding to the minimal score, to the shape corresponding to the maximal score (B: PC1; C: PC2). D. Means of the geographic group in the morphospace defined by the first two axes of a bgPCA. Distance between grid bars: d=0.02. Abbreviations: cf. Table 1.

Figure 6. Allometric shape differentiation of the first upper molar. A. Allometric shape variation. Size is estimated by the centroid size of the UM1; shape by the Common Allometric Component (CAC). "C" indicates the Chadian specimen in the Sahara sample. B. Allometric deformation. Arrows point from the shape corresponding to the minimal centroid size, to the shape corresponding to the maximal centroid size. C. Means of the geographic group in the morphospace defined by the first two axes of a bgPCA on the residuals of a regression of the aligned coordinates vs. size. Distance between grid bars: d=0.02.

Figure 7. Karyotypic variation of *Acomys cahirinus* s.l. in the Eastern Mediterranean area. The pie charts indicate the proportion of the 2*n* numbers in the different populations. Data from Giagia-Athanasopoulou et al. (2011).

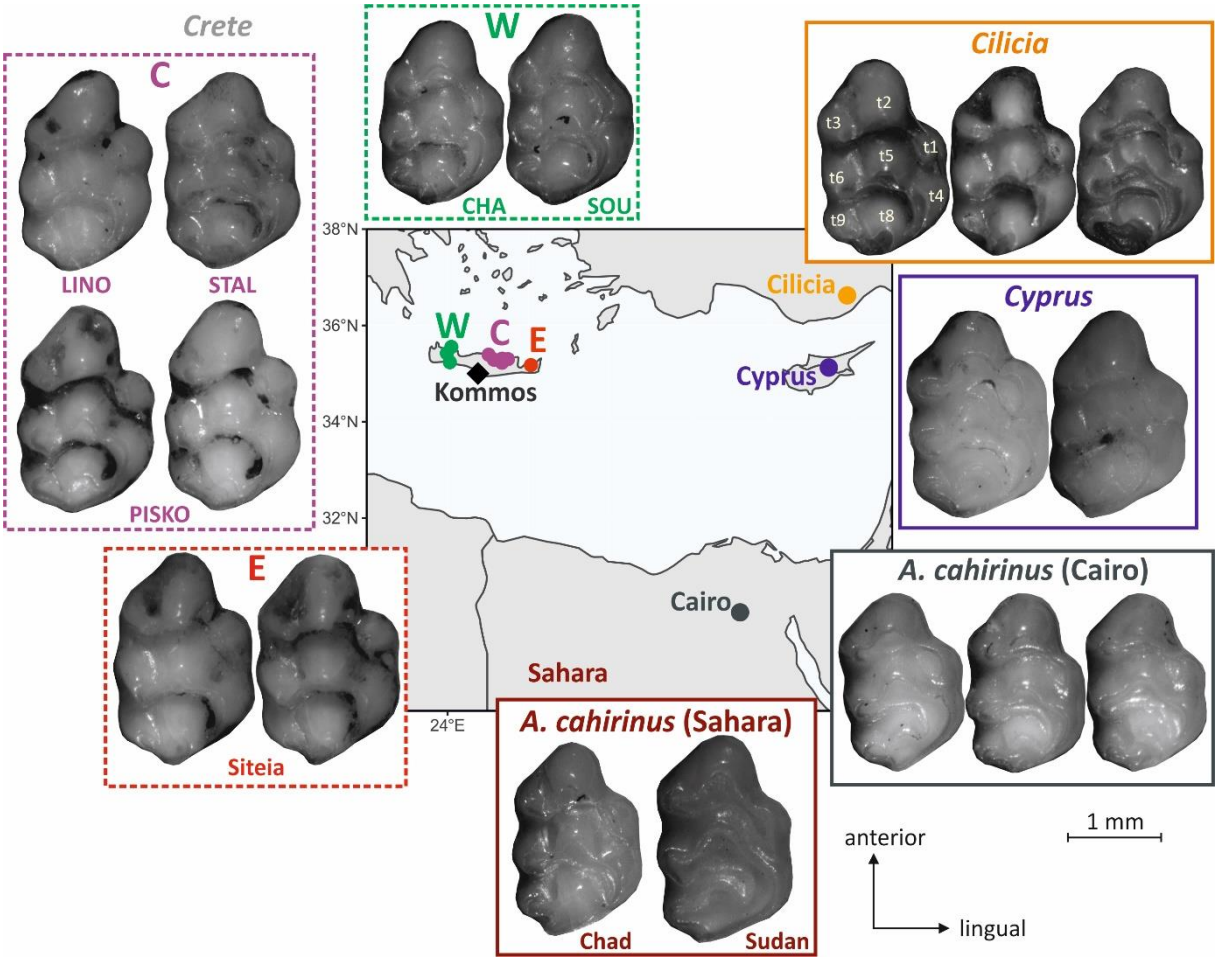

Figure 1. Sampling localities and examples of first upper molars (UM1) in the various populations of *Acomys* considered in this study. All belong to the *cahirinus s.l.* group. Spiny mice from the island of Crete are designated as *A. minous*, those from the island of Cyprus as *A. nesiotes* and those confined to a small area in Cilicia (Asia Minor, Turkey) as *A. cilicicus*. Nomenclature of the cusps is indicated on one molar tooth of *A. cilicicus*. The boxes indicate the color code of the areas in figures for morphometrics. For abbreviations of some localities (LINO, STAL, PISKO) see Table 1. All teeth to the same scale (scale bar bottom right).

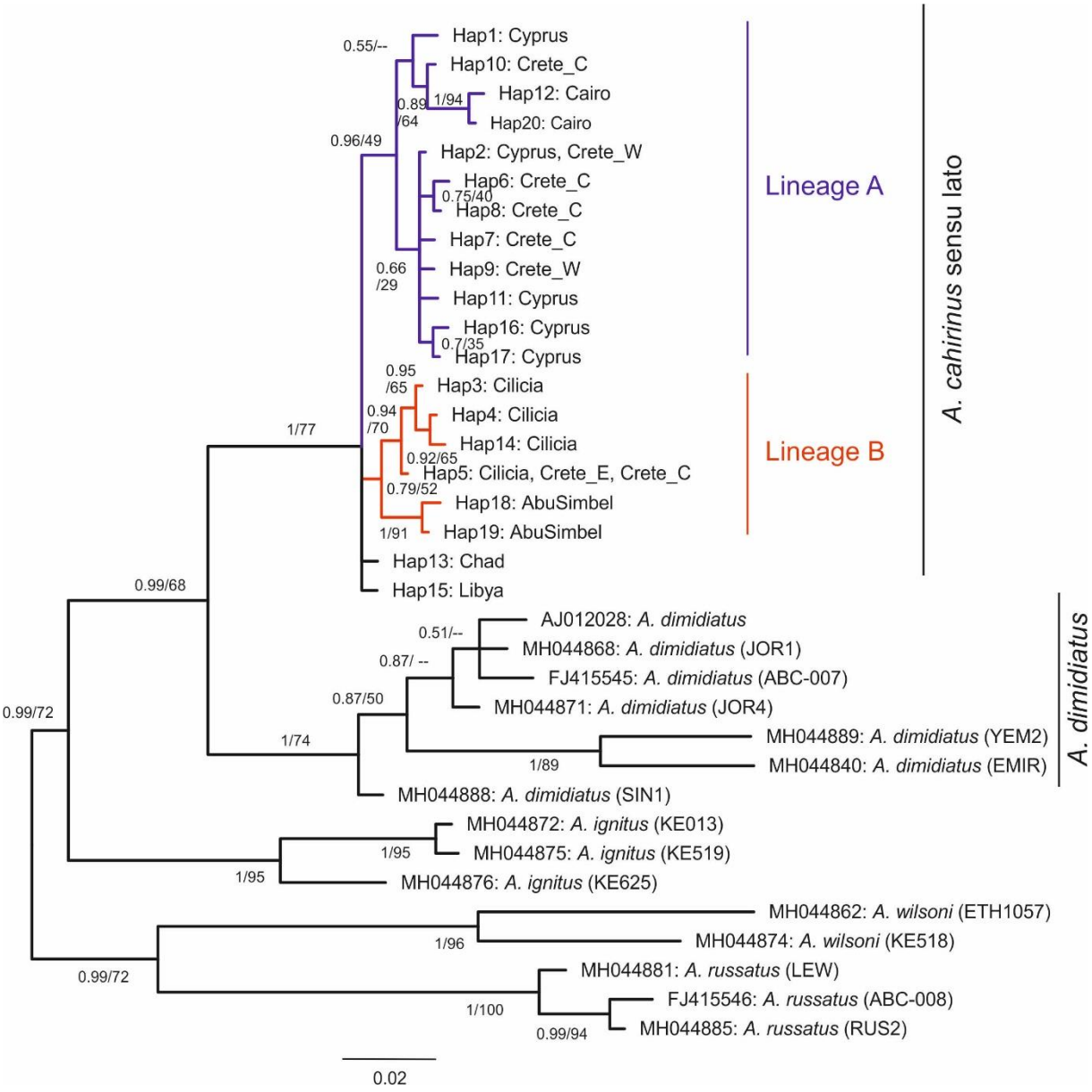

Figure 2. Bayesian phylogeny of D-loop haplotypes of *Acomys cahirinus sensu lato* (i.e. including *A. minous, A. nesiotes* and *A. cilicicus*). Posterior probability and bootstrap support are indicated for each node. " – " indicates that the node is not supported in the phylogeny reconstructed with PhyML.

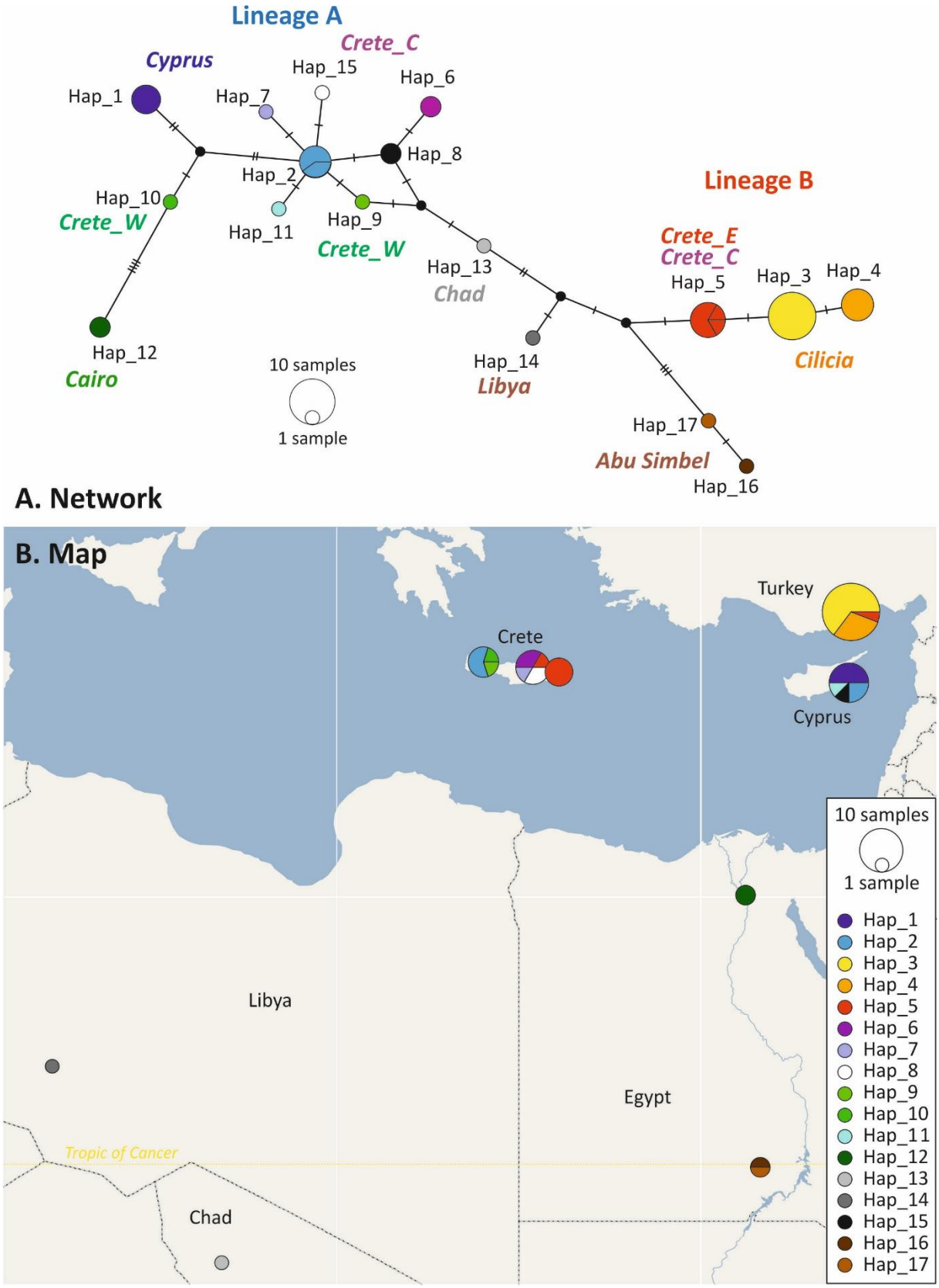

Figure 3. Network and geographic distribution of the D-loop haplotypes. A. Median-joining haplotype network. B. Geographic repartition of the haplotypes. Each haplotype is identified by the same color code on both figures.

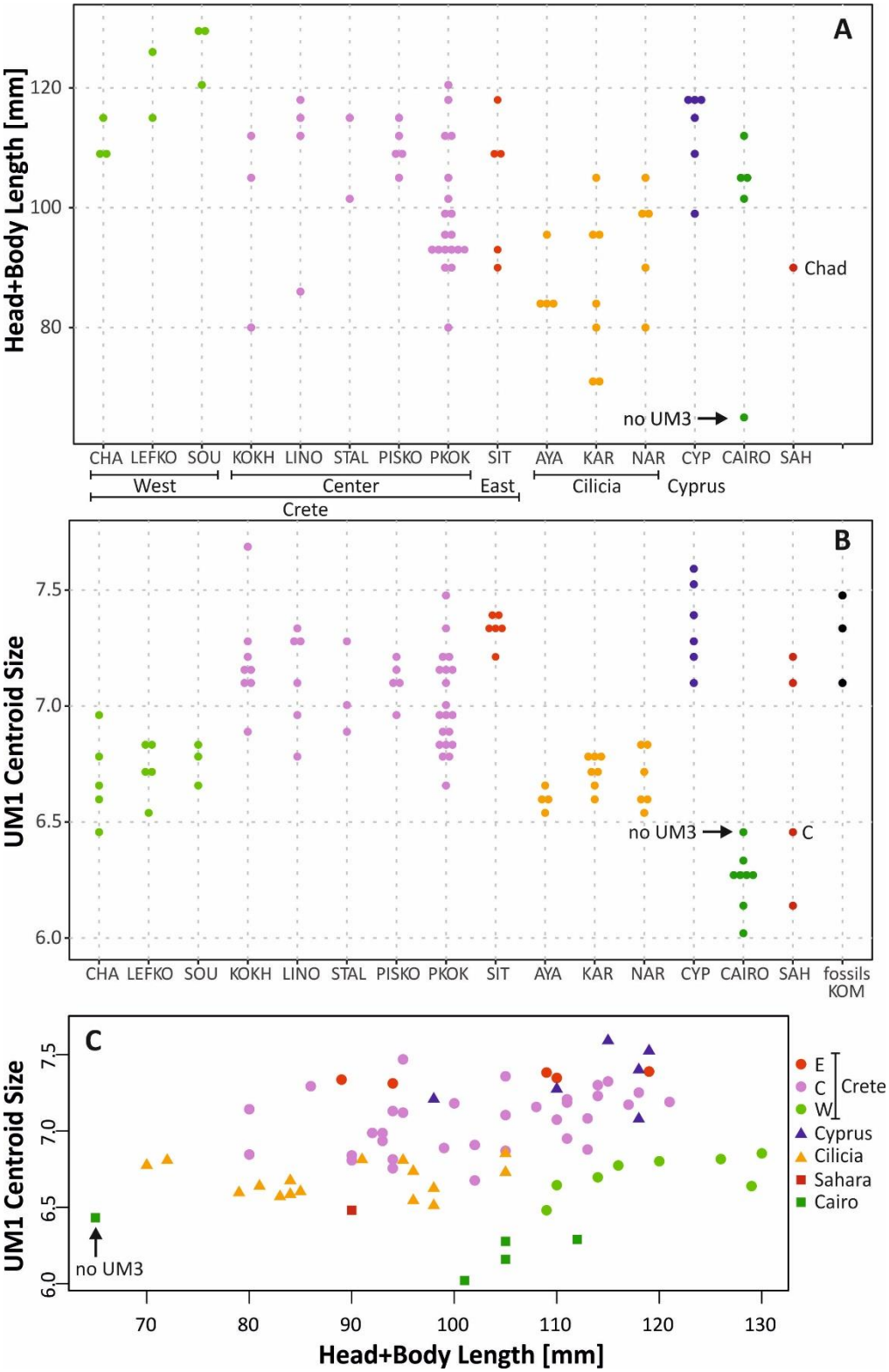

725

726 **Figure 4**. Size variation of *Acomys cahirinus* s.l. A. Body size (Head + Body Length) in the modern
727 populations from Crete, Cyprus, Turkey, Cairo and Sahara. B. Size of the first upper molar (UM1) in the
728 same populations; fossils from Kommos (Iron Age, Crete) are also included. C. Relationship between
729 body and molar size. The Chadian specimen among the Sahara sample is indicated by "Chad" or "C".
730 The arrow with "No UM3" points to a young specimen without erupted third molar.

731

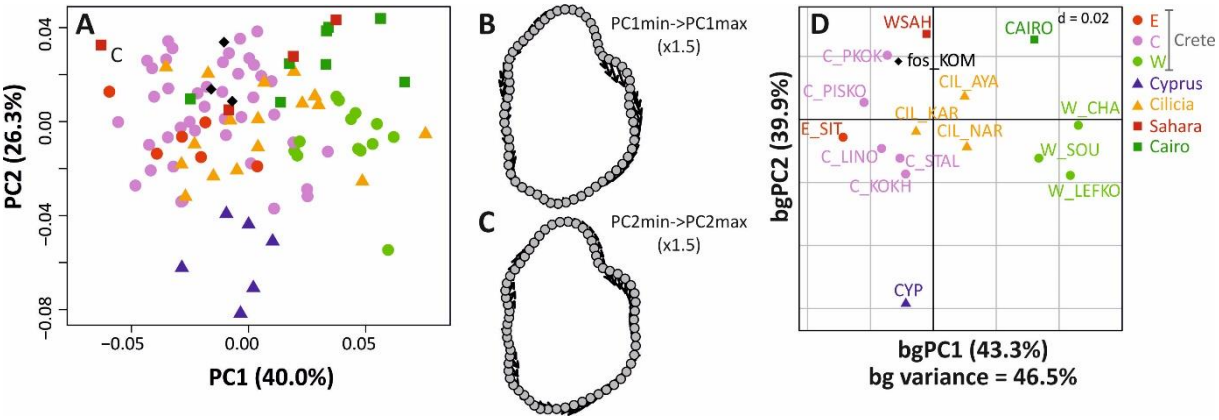

Figure 5. Shape differentiation of the first upper molar between the different populations of *Acomys cahirinus* s.l., including the fossil teeth from Kommos (Iron Age, Crete). A. Morphospace defined by the first two axes of a PCA on the aligned coordinates of the points delineating the outline of the first upper molar. Each dot corresponds to a tooth. "C" indicates the Chadian specimen among the Sahara sample. B, C: Deformation along the PC axes. Arrows point from the shape corresponding to the minimal score, to the shape corresponding to the maximal score (B: PC1; C: PC2). D. Means of the geographic group in the morphospace defined by the first two axes of a bgPCA. Distance between grid bars: d=0.02. Abbreviations: cf. Table 1.

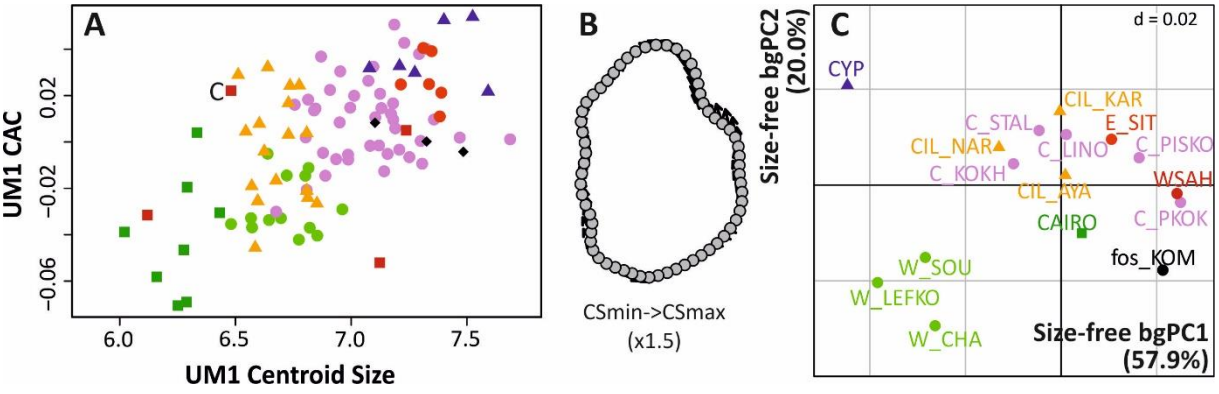

Figure 6. Allometric shape differentiation of the first upper molar shape. A. Allometric shape variation. Size is estimated by the centroid size of the UM1; shape by the Common Allometric Component (CAC). "C" indicates the Chadian specimen among the Sahara sample. B. Allometric deformation. Arrows point from the shape corresponding to the minimal centroid size, to the shape corresponding to the maximal centroid size. C. Means of the geographic group in the morphospace defined by the first two axes of a bgPCA on the residuals of a regression of the aligned coordinates vs. size. Distance between grid bars: d=0.02.

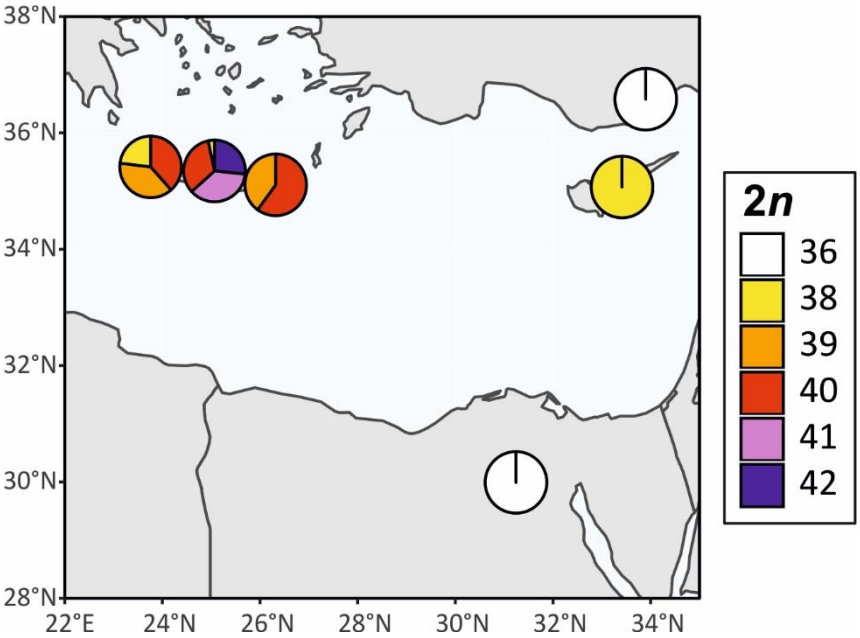

Figure 7. Karyotypic variation of *Acomys cahirinus* s.l. in the Eastern Mediterranean area. The pie charts indicate the proportion of the 2*n* numbers in the different populations. Data from Giagia-Athanasopoulou et al. (2011).

763 **Supplementary Informations**

764

765 **Supplementary Figure 1.** Chronogram obtained with BEAST. Values on the nodes represent medians
766 of estimated divergence date, and the horizontal bars show 95% highest posterior density of these
767 estimates. Red stars indicate the positions of three fossil constrains used for the calibration of
768 molecular clock.

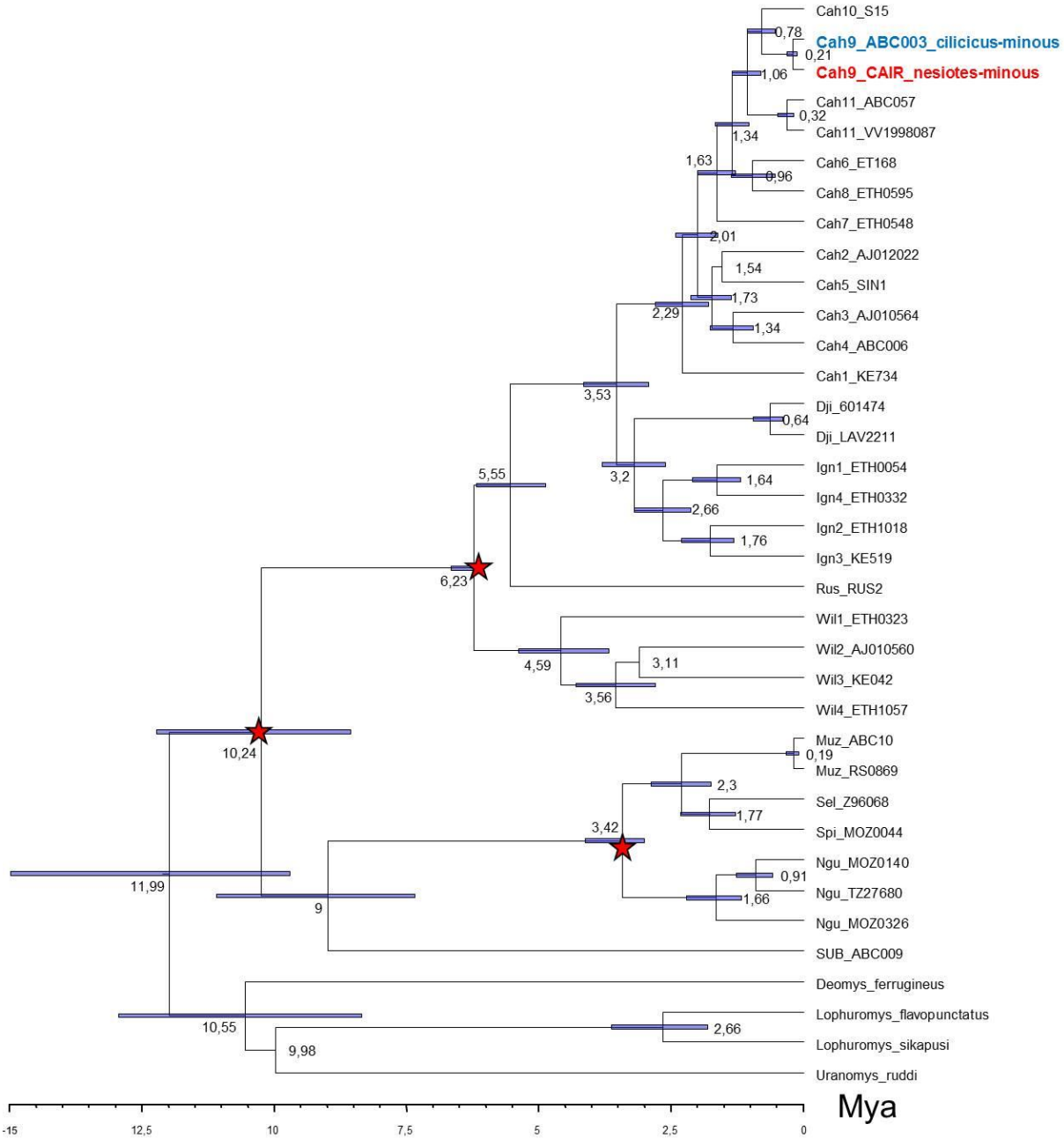

769

770

771

772 **Supplementary Table 1**. Accessions of the sequences used in the dating analysis. Lineages and
773 groups defined as in Aghova et al. (2019).
774

Genus	Species	Lineage	Group	Cytb	D-loop	IRBP	RAG1
Acomys	*cineraceus*	*Cah1*	*cahirinus*	MH044976	MH044879	MH044739	MH044833
Acomys	sp. 2	*Cah2*	*cahirinus*	AJ012022			
Acomys	sp. 1	*Cah3*	*cahirinus*	AJ010564			
Acomys	*johannis*	*Cah4*	*cahirinus*	FJ415483	FJ415544	MH044740	MH044818
Acomys	*dimidiatus*	*Cah5*	*cahirinus*	MH044985	MH044888	MH044767	MH044829
Acomys	*mullah*	*Cah6*	*cahirinus*	MH044992	MH044845	MH044742	MH044834
Acomys	sp. B	*Cah7*	*cahirinus*	KX290493	MH044857	MH044764	MH044826
Acomys	sp. A	*Cah8*	*cahirinus*	MH045013	MH044858	MH044761	MH044836
Acomys	***cahirinus***	***Cah9_Lineage A***	***cahirinus***	**MH045014**	**MH044837**	**MH044772**	**MH044832**
Acomys	***cahirinus***	***Cah9_Lineage B***	***cahirinus***	**FJ415480**	**FJ415541**	**MH044773**	**MH044831**
Acomys	sp. Cah10	*Cah10*	*cahirinus*	MH045016		MH044753	MH044817
Acomys	*chudeaui*	*Cah11*	*cahirinus*	FJ415534	FJ415595		
Acomys	*chudeaui*	*Cah11*	*cahirinus*	MH045006		MH044755	MH044822
Acomys	*louisae*	*Dji*	*cahirinus*	MH044903			MH044805
Acomys	*louisae*	*Dji*	*cahirinus*	MH044900		MH044735	
Acomys	sp. C	*Ign1*	*cahirinus*	MH045020	MH044850	MH044747	MH044813
Acomys	sp. Ign2	*Ign2*	*cahirinus*	MH044971	MH044859	MH044743	MH044807
Acomys	*ignitus*	*Ign3*	*cahirinus*	MH044968	MH044875	MH044756	MH044812
Acomys	*kempi*	*Ign4*	*cahirinus*	MH045033	MH044855	MH044744	MH044809
Acomys	*russatus*	*Rus*	*russatus*	MH044905	MH044885	MH044733	MH044788
Acomys	*muzei*	*Muz*	*spinosissimus*	FJ415487	FJ415548		
Acomys	*muzei*	*Muz*	*spinosissimus*	MG434400		MG434355	
Acomys	*ngurui*	*Ngu*	*spinosissimus*	MG434388		MG434353	
Acomys	*ngurui*	*Ngu*	*spinosissimus*	MG434396		MG434354	
Acomys	*ngurui*	*Ngu*	*spinosissimus*	MG434414		MG434358	
Acomys	*selousi*	*Sel*	*spinosissimus*	Z96068			
Acomys	*spinosissimus*	*Spi*	*spinosissimus*	MG434385		MG434352	
Acomys	*subspinosus*	*Sub*	*subspinosus*	FJ415486	FJ415547	MH044731	MH044787
Acomys	*percivali*	*Wil1*	*wilsoni*	MH044950	MH044854	MH044783	MH044792
Acomys	sp. 'Magadi'	*Wil2*	*wilsoni*	AJ010560			
Acomys	aff. *percivali*	*Wil3*	*wilsoni*	MH044911	MH044873	MH044780	MH044795
Acomys	*wilsoni*	*Wil4*	*wilsoni*	MH044912	MH044862	MH044774	MH044797
Deomys	*ferrugineus*		OUTGROUP	FJ415478	FJ415539	AY326084	
Lophuromys	*flavopunctatus*		OUTGROUP	EU349754		AY326091	AY294950
Lophuromys	*sikapusi*		OUTGROUP	AJ012023		AJ698899	KC953515
Uranomys	*ruddi*		OUTGROUP	HM635858	FJ415540	EU360812	DQ023454

775

776

777

Subset	Best Model	Sites number	Partition names
1	TRN+I+G	335	Cytb_pos1
2	HKY+I+G	335	Cytb_pos2
3	HKY+G	335	Cytb_pos3
4	K80+I	1319	IRBP_pos3, RAG1_pos1, RAG1_pos2, IRBP_pos1
5	HKY+G	659	IRBP_pos2, RAG1_pos3
6	HKY+I+G	526	Dloop

778

779 **Supplementary Table 2.** Substitution models used in the BEAST analysis.

780

781